FRACTURE TOUGHNESS DETERMINATION OF COMPOSITES BASED ON ALUMINA FROM INDENTATION-INDUCED VICKERS CRACKS

Magdalena Szutkowska

The Institute of Metal Cutting, Cracow, Poland, email:szutkows@ios.krakow.pl

ABSTRACT

The modified indentation technique for measurement of fracture toughness by indentation induced controlled Vickers crack growth in bending (ICVC) and indentation strength in bending (ISB) method have been presented. For the comparison the indentation test was performed by the direct crack measurement (DCM) method. Relationship of in-plane and out-of- plane displacements and strain distribution nearby Vickers hardness indentation and cracks with the K_{IC} was analysed by means of automated grating (moiré) interferometry (GMI) method. Tool ceramic composites: alumina-zirconia and alumina reinforced with Ti(C,N) were tested.

1.INTRODUCTION

Efforts made during the last decade have resulted in a remarkable progress in the properties of brittle matrix composites (BMC). Such materials should exhibit high hardness and wear resistance, high melting temperature, oxidation resistance, chemical stability, creep deformation resistance, thermal shock resistance and sufficient levels of strength and fracture toughness-1. Brittle matrix composites based on alumina fulfill the most of these requirements and are already used as a tool ceramic material. Development in ceramic cutting tools is caused by the requirement for high reliability in automated manufacturing lines and the substitution of certain grinding operations by highly precise cutting approaches-2. Taking into account these demands the investigations of precise cutting operations were oriented on ceramic composites based on alumina: alumina-zirconia and alumina reinforced with Ti(C,N). The main advantage of such tools is possibility of ecological "dry cutting" without application of cutting fluids. In spite of many attractive properties of ceramic composites based on alumina one of the primary disadvantage is their brittle nature, characterized by low fracture toughness. Considering a various approach to determine the fracture toughness of alumina composites a greater attention was paid on the indentation methods. These methods fall into two main tests in which K_{IC} is evaluated from direct measurements of crack size as a function of indentation load and from a strength measurement, where the indentation crack serves as a controlled flaw in a bending specimen. Numerous specimen geometries and experimental methods has been proposed and adopted to determine the fracture toughness of ceramic composites. But up to now universally agreed standard for fracture toughness das not exist. There are now a very large number of theoretical models in the literature relating the surface cracks measured after indentation to the indenter load and material parameters: Young's modulus, hardness and fracture toughness-3. There is still considerable debate as to the nature of the cracks observed around a Vickers indentation. The most commonly used crack systems produced by a Vickers hardness indenter show Figures 1a to 1 d. The Palmqvist cracks form at apexes of the indentation impression remaining connected to the surface. Median cracks are generated beneath the indentation impression (Fig.1b). They are in the shape of penny and lies on a plane of symmetry containing the contact axis. Upon complete removal of the indenter, the radial and median cracks sometimes meet to form half-penny cracks (Fig. 1c). During unloading at high indentation loads, lateral cracks (Fig.1d) may nucleate beneath the indenter and propagate sideways in a circular form, which may divert upwards towards the surface and cause chipping. In addition to the above commonly observed crack systems, other variant crack systems could also be produced by the Vickers indentation. They include secondary Palmqvist cracks (Fig.1e) and shallow lateral cracks (Fig.1f), which emanate from the edge of the

indentation impression in some cases. The former usually occurs at small indentation loads in large-grained materials, while the latter at high indentation loads-4.

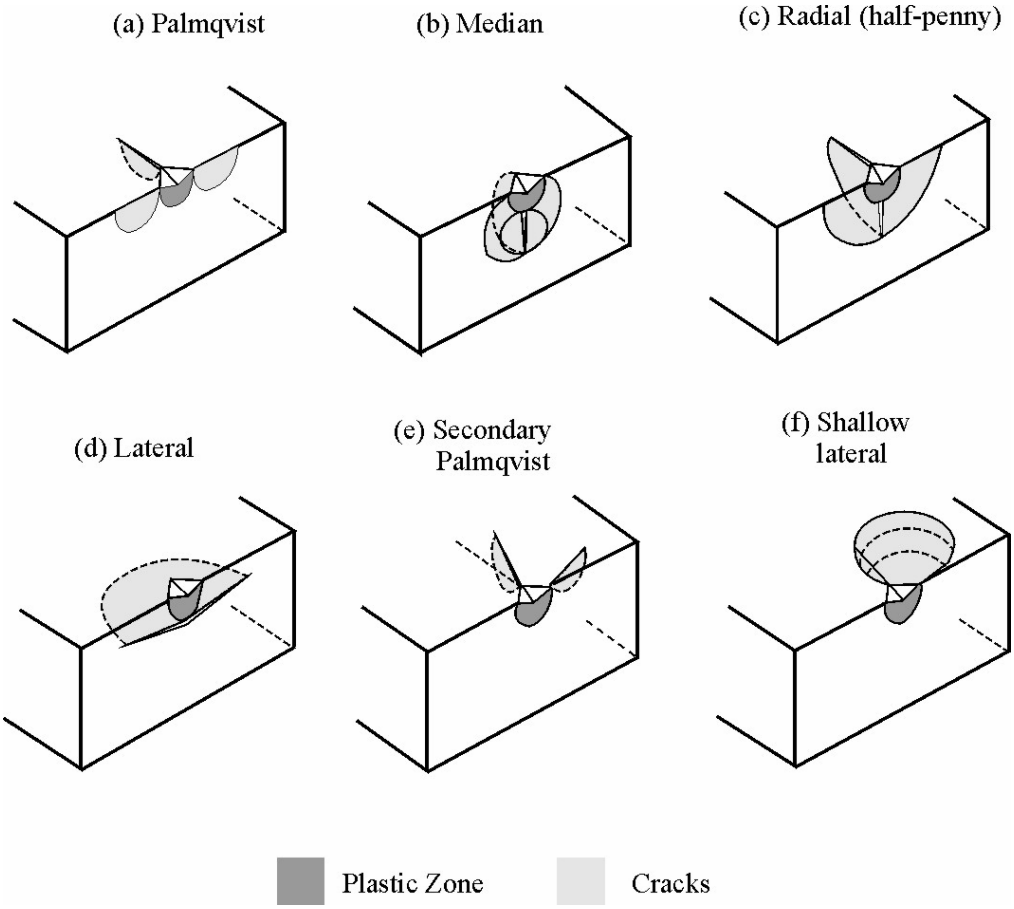

Fig.1. Primary (a,b,c,d) and secondary (e,f) crack systems produced by the Vickers hardness indentation in ceramics-4.

Both the Palmqvist and median/radial cracks emanated from the corner of the Vickers hardness indentation provide base to determination the indentation fracture toughness. In any indentation fracture toughness determination a critical stress intensity factor is a proper accounting of the residual contact stresses in the fracture mechanics formulas. These stresses play primary role in driving the cracks at all stages of growth both during and after the indentation cycle. The modified indentation technique for measurement of fracture toughness by indentation induced controlled Vickers crack growth in bending (ICVC) and indentation strength in bending method (ISB) was carried in the work. For the comparison the indentation test was performed by the direct crack measurement (DCM) method as well. In general, indentation technique has certain advantages compared with the conventional method because the experimental procedure is straightforward, involving minimal specimen preparation and small amount of material.

2. EXPERIMENTAL PROCEDURE

The tests were performed on the composites based on alumina: Al_2O_3-10 wt% ZrO_2 (unstabilized ZrO_2), Al_2O_3-10 wt% ZrO_2 (3 mol%Y_2O_3 stabilized ZrO_2) and Al_2O_3/(30 wt% TiC+TiN) with 2 wt% ZrO_2. The samples were fabricated using commercial alumina powder type A16SG produced by the Alcoa firm. The alumina powder contains 90% of α-phase with 99.8% purity with mean particle size smaller than 0.5 μm. Sintering additives, such the MgO to inhibit grain growth have been introduced. Specific surface of alumina particle determined by nitrogen absorption at the

temperature of liquid nitrogen is S_{BET}=4.54 m^2/g. The specific surface of the tested powders for pure zirconia is S_{BET}=4.13 m^2/g and for3 mol% yttria stabilized zirconia is S_{BET}=4.70 m^2/g respectively. The pure zirconia was obtained by precipitation from water solution of $ZrOCl_2$ by means of water solution of ammonia. Solid solution of 3 mol% yttria doped zirconia has been obtained by co-precipitation from the common aqueous solution of the $ZrOCl_2$ +YCl_3. This solution was carried to intensively mixed ammonia aqueous solution. After roasting zirconia has been milling in mixer mill in denatured alcohol medium. Green plates with dimensions of 60.0 ×70.0 ×7.0 mm were uniaxially pressed at 50 MPa and then cold isostatically pressed at 250 MPa. The alumina-zirconia composites were sintered in the high temperature electric furnace of Seco-Warwick firm at the maximum temperature 1923 K. Alumina powder was blended together with 30 wt% TiC+TiN commercial powder and 2 wt% ZrO_2. These specimens were sintered in a high temperature vacuum furnace of the Balzers firm at temperature beneath 1973 K. The Vickers hardness indentation was produced in centre of 4 mm wide polished face using a 200 N load. Surface of the tested samples designed for indentation through 3 μm diamond suspension DP Spray using standard techniques was polished. Specimens were oriented in such way that one of they indent diagonals were perpendicular to the sample edges. The samples were subjected to three-point bending test with support span S = 40 mm using the universal testing machine Zwick 1446 with rate v = 0.005 mm/min. After reloading of the specimen the crack length was measured with microscopical objective heads in horizontal configuration and then it was repeated up to failure of the specimen or extension of the one of the cracks to length more than 1 mm. If the external stress field σ is applied to the indented specimen, the total stress intensity factor K_T (sometimes called effective stress intensity factor) is the sum of the residual stress intensity factor K_{RD} and the applied stress intensity factor K_A. The K_T can be expressed by equilibrium equation (1)-5:

$$K_T = K_{RD} + K_A = \chi P c^{-3/2} + \psi \sigma c^{1/2} \quad (1)$$

where: P is the indentation load, c is the surface crack length, $\chi = \xi(E/H)^{1/2}$ is the dimensionless parameter characterizing the integrated affect of the residual indentation stress field over the half-penny crack, E is the Young's modulus, H is the hardness, ψ is the dimensionless crack geometry factor, σ is the applied stress. The residual stress field arises from the residual strain-mismatch of the plasticity deformed indentation constant zone imbedded in the surrounding elastically restraining matrix is represented by K_{RD}. When σ increases and the instability condition i.e. $K_T=K_{IC}$ is reached, crack undergoes stable growth before the final failure. The regime of stable crack extension between the initial crack length c_o and instability crack length c_m allows to obtain an experimental crack extension curve and to get the χ and the K_{IC} values. Equation (4) can be rearrenged into (2):

$$\psi \sigma c^2 / P = K_{IC} c^{3/2} / P - \chi \quad (2)$$

The terms $X= c^{3/2} / P$ and $Y=\psi \sigma c^2 / P$ can be determined experimentally. Thus the K_{IC} and residual stress factor χ are obtained from the slope and the intercept of the interpolating function respectively. The coefficient ψ was calculated from equation given in-5. In the ISB method the specimen with Vickers cracks is loaded at the higher speed 1 mm/min and K_{IC} is evaluated during unstable crack growth. Fracture toughness is calculated from simple formula (3) proposed by Chantikul-6 for the median/radial shape of cracks:

$$K_{IC} = 0.59(E/H)^{1/8} (\sigma P^{1/3})^{3/4} \quad (3)$$

where: σ is the failure stress, P is the loading force of Vickers hardness indenter.

The specimens with dimensions 2.5×4.0×25.0 mm obtained after ISB test were used for indentation test. The measurements of the indentation fracture toughness at different loads of the Vickers hardness indenter, starting from 9.81 N; 49.5 N; 98.1 N; 294.3 N; 495.0 N up to 981.0 N were carried. A correlation between the fracture toughness and ratio of cracks to indent size was expressed according to selected equations proposed by different authors: Langford-7, Niihara-8, Laugier-9, Anstsis-10, Liang-11 and Lawn-12. On the basis of an own experience-13, fracture

toughness K_{IC} calculated by Niihara's equation (4) was used for comparison. In this case, relation between the fracture toughness and a ratio of cracks to indent size at the condition $c/a \geq 2.5$ is expressed by the equation (4):

$$(K_{IC}\, \varphi / H\, a^{1/2})\, (H/E\, \varphi)^{2/5} = 0.129\, (c/a)^{-3/2} \qquad (4)$$

where: K_{IC} is the critical stress intensity factor, φ is the constrain factor, H is the Vickers hardness, E is the Young's modulus, a-half of indent diagonal.

The right side of equation (4) is equal 0,035 $(c/a)^{-1/2}$ for Palmqvist type of cracks. The specimens were indented on the polished surface with Vickers hardness tester using loads from 9.81N to 490.5 N. Serial sectioning was used to determine the indent crack profiles in the samples. Special staining technique with drop of saturated lead acetate solution was used to better revealing of the crack profile. The regions on the fracture surfaces were observed using scanning electron microscopy (SEM). Evaluation of chipping compliance of tested ceramics subjected different loading forces was carried by using of Zeiss optical microscope equipped with Dick Nomarski device. Young's modulus by means of dynamic method was determined using frequency elastometer. Defect structures near the indentation tip and cracks initiated within zone of plastic deformation beneath the Vickers indentation were observed on the cross-sectional view of specimen by means of transmission electron microscopy (TEM) Philips CM20 TWIN at 200kV. For this reason thin foil specimen was prepared from the bulk material with contained Vickers hardness indentations at loading force 98,1N. Thin foil was prepared through mechanical polishing and ion milling with Gatan DuoMill 600. Out-of-plane and in-plane displacements and strain distribution in the range of Vickers indentations and nearby the median/radial cracks were measured by means of automatic grating (moiré) interferometry (GMI) method. 3-Dimensional plots of out-of plane displacements and strain distribution were observed with Twyman-Green interferometer. For this purpose, a diffraction grating 1200 l/mm was glutted on the specimen.

3.RESULTS & DISCUSSION

Data from more than twenty measurement points determined by indentation induced controlled Vickers crack growth in bending methods (ICVC) allow to obtain plots with relationship of parameter $Y = \psi\, \sigma\, c^2 / P$ versus $X = c^{3/2}/P$ for tested composites (Fig.2). The K_{IC} value determined from the slope of strain line exhibits higher value of K_{IC} (about 20%) for alumina–10 wt% zirconia composite with unstabilized zirconia in comparison to alumina-10 wt% zirconia composite with 3 mol% yttria stabilized zirconia and Al_2O_3-30 wt% TiC+TiN with 2 wt% ZrO_2 composite. Residual stress factor χ obtained from the intersection of the interpolating function with (Y) axis includes in the range (0.063-0.074). The Al_2O_3-30wt% TiC+TiN with 2wt% ZrO_2 composite characterises itself the highest value of the residual stress factor χ.

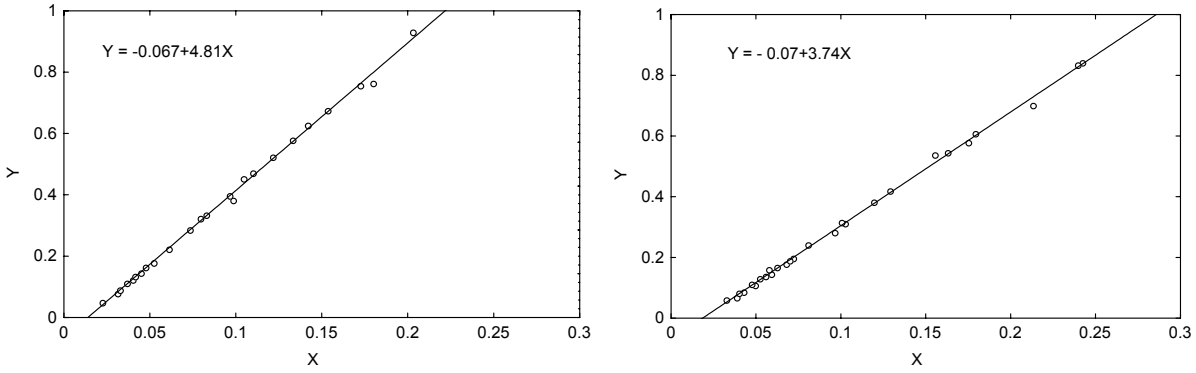

Fig.2. Relationship of $X = c^{3/2}/P$ and $Y = \psi\, \sigma\, c^2 / P$ for a) Al_2O_3-10 wt% ZrO_2 (with unstabilized zirconia), b) Al_2O_3-30 wt% TiC+TiN with 2 wt% ZrO_2

Summary results of the fracture toughness K_{IC} measured by means of indentation induced controlled Vickers crack growth in bending (ICVC) and indentation strength in bending (ISB) are presented in Table 1.

Table 1. The fracture toughness K_{IC} obtained by indentation induced controlled Vickers crack growth in bending (ICVC) method, residual stress factor χ and K_{IC} obtained by (ISB) method.

Ceramic composites	K_{Ic} (ICVC) [$MPam^{1/2}$]	Residual stress factor χ	K_{Ic} (ISB) [$MPam^{1/2}$]
Al_2O_3-10 wt% ZrO_2 (unstabilized)	4.81±0.04	0.067± 0.004	5.24±0.12
Al_2O_3-10 wt% ZrO_2 (3 mol% yttria stabilized.)	3.77±0.04	0.063±0.005	4.14±0.13
Al_2O_3-30 wt% TiC+TiN with 2 wt% ZrO_2	3.74±0.03	0.070±0.003	4.22±0.19

Fracture toughness K_{IC} obtained by three point bending of the specimen with Vickers crack during its unstable growth (ISB method) is somewhat higher than K_{IC} determined by indentation induced controlled Vickers crack growth in bending (ICVC method). This difference comes to about 10%. Both methods give the same relationship K_{IC} versus kind of tested composites. Alumina –zirconia composite with unstabilized ZrO_2 exibits the highest value of K_{IC} for the presented methods. It can be explain by analysis of phase composition of the alumina–zirconia composites. Analysis of the Raman spectrum reveals presence about of 25vol% of monoclinic zirconia phase and 75 vol% of tetragonal phase in alumina–10 wt% zirconia composite with unstabilized zirconia. In alumina-10 wt% zirconia with 3 mol% yttria stabilized zirconia only tetragonal phase is observed. The ISB method can be used to determine fracture toughness at the assumption that induced Vickers cracks are median/radial type. On the contrary, results are significantly overstated and differ from real values. Observations of the interaction between the crack path and microstructure on the extended cracks of Vickers indentation for tested ceramic composites were made. SEM micrograph of typical crack profiles in Al_2O_3-30wt% TiC+TiN with 2wt% ZrO_2 and alumina–10wt% zirconia composite with unstabilized zirconia are illustrated in Fig.3 and Fig.4. Corresponding SEM micrograph of the Al_2O_3-30 wt% TiC+TiN with 2 wt% ZrO_2 composite (Fig.3) confirms the predominantly straight transgranular and limited intergranular character of crack path. In alumina-zirconia composites diverse character of crack propagation is observed. The intergranular crack path for alumina–10 wt% zirconia composite with unstabilized zirconia is noticed (Fig.4). In contrast, crack path in the alumina-10 wt% zirconia with 3 mol% yttria stabilized zirconia is almost exclusive transgranular, with no indication of crack deflection or wake bridging. Diversions in morphology of crack profiles in tested composites influence on fracture toughness K_{IC}.

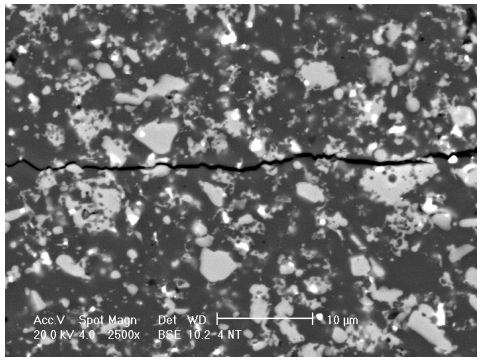

Fig.3. SEM micrograph of Vickers crack profile on the surface of the Al_2O_3-30 wt% TiC+TiN with 2wt% ZrO_2 composite.

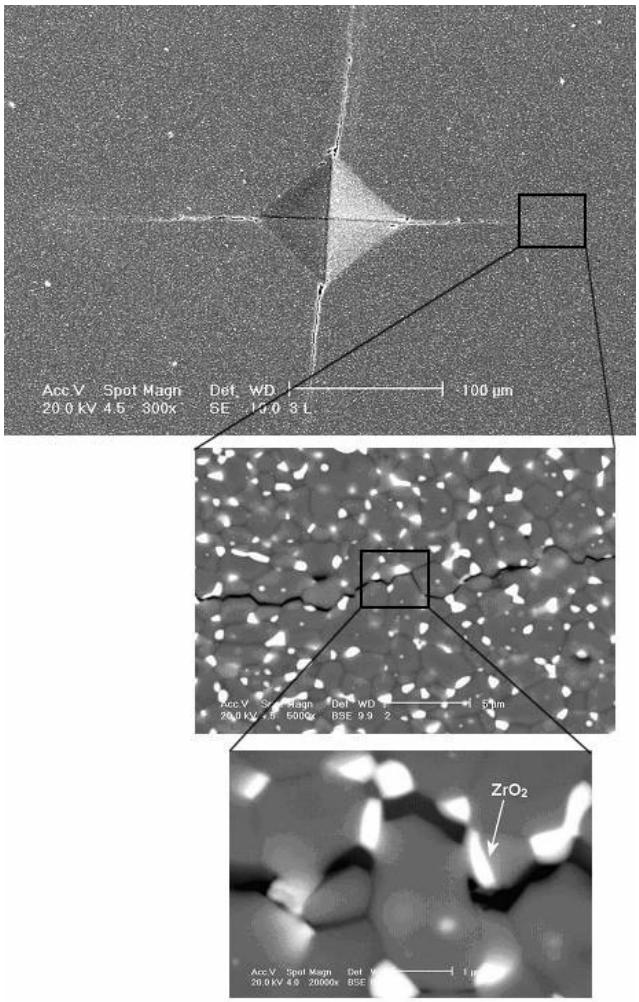

Fig.4. SEM micrograph of the Vickers hardness indentation with crack profile on the surface of the alumina–10 wt% zirconia composite with unstabilized zirconia.

Summary of the indentation fracture toughness K_{IC} determined according to selected formulae presented by various authors-7,8,9,10,11,12 are shown in the Figure 5.

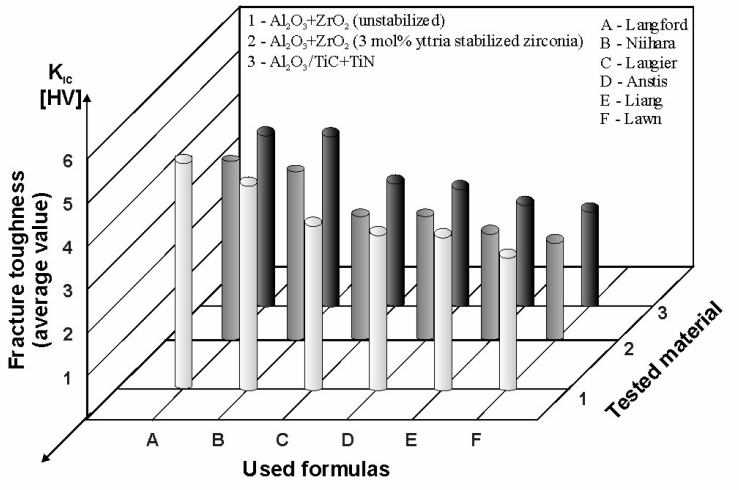

Fig.5. Summary of the indentation fracture toughness K_{IC} determined according to selected formulae presented by various authors-7,8,9,10,11,12.

As indicated in Figure 5 obtained results allow to observe strong relationship of K_{IC} in dependence on formulae accepted to calculations. A difference between the lowest and highest value of K_{IC} is about 50%. The highest value of K_{IC} is calculated with using the Langford's-7 'universal' equation and is applied regardless of type of cracks, while the lowest value of K_{IC} is for the Lawn's-12 equation. The nearest to conventional fracture toughness (SENB specimen) is K_{IC} determined by equation (4)-13. Observations of the lateral crack behavior nearby the Vickers hardness indentation allow to estimate a chipping resistance of the tested ceramic composites. For this purpose various loading force from 9.81 N to 981N has been applied to the Vickers hardness indenter. The chippings, which arise nearby the Vickers indentation are related with loading force and kind of tested ceramics. The single chipping from the loading force 490.5 N is observed for the Al_2O_3-30wt% TiC+TiN with 2wt% ZrO_2 composite only. When the loading force increases up to 981 N deep lateral cracks and double or sometimes multi-chippings are formed (Fig.6a). For the alumina-zirconia composites shallow lateral cracks without chipping are only visible at indentation load 981 N (Fig.6b).

a) b)

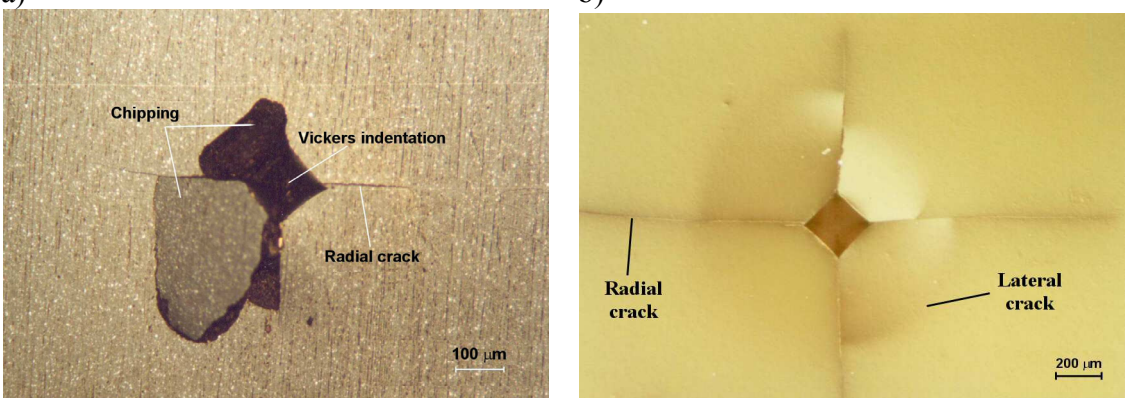

Fig.6. Examples of cracks and chippings in ceramic composites based on alumina produced at indentation load 981 N: a) Al_2O_3-30 wt% TiC+TiN with 2 wt% ZrO_2, b) Al_2O_3-10 wt% ZrO_2 (with unstabilized zirconia).

Structure of the composites in a zone adjacent to the Vickers indentation produced at 98.1 N loading force beneath the indentation tip was observed on the cross-section by means of transmission electron microscopy TEM. Effect of such loading force generates the deformation by dislocation slips and microtwinnings. Examples of electron micrographs in the zone beneath the Vickers indenter tip with visible dislocations and corresponding electron diffraction pattern are presented in Figure 7.

a) b)

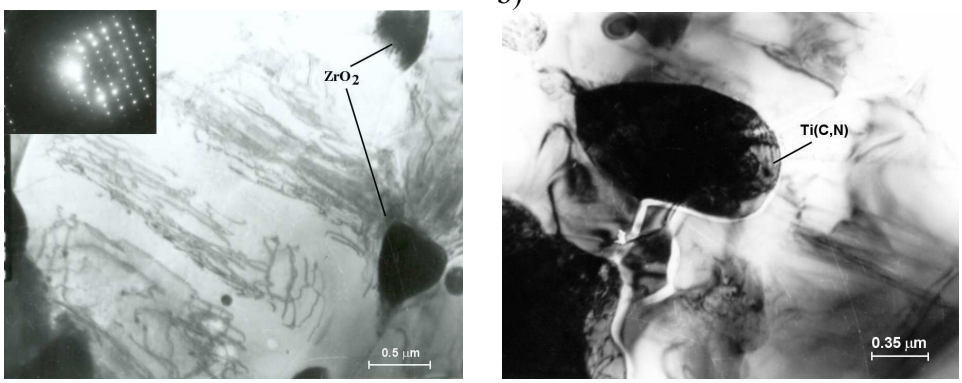

Fig.7. Electron micrographs in the zone beneath the Vickers indenter tip of: a) Al_2O_3-10 wt% ZrO_2 (with unstabilized zirconia), b) Al_2O_3-30 wt% TiC+TiN with 2 wt% ZrO_2.

Summary of the fracture toughness (K_{IC}) of alumina-10 wt% zirconia composites, alumina reinforced with TiC+TiN composite tested by means of different methods: indentation induced controlled Vickers crack growth in bending (ICVC), indentation strength in bending (ISB) and direct crack measurement (DCM) is shown in Figure 8.

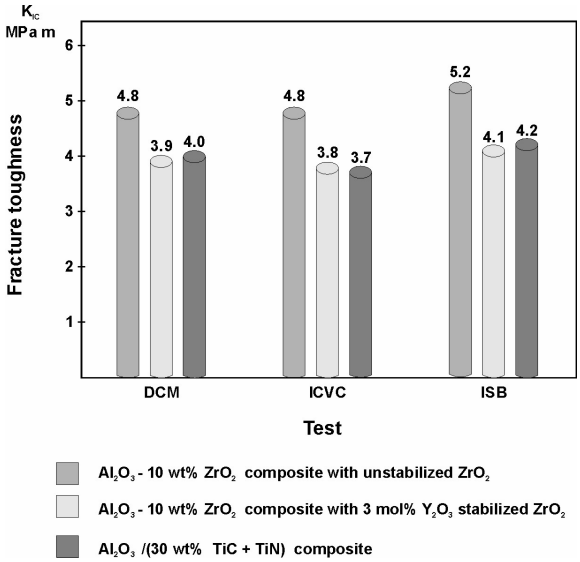

Fig.8. Comparison of the fracture toughness (K_{IC}) determined by means of the indentation methods: direct crack measurement (DCM), indentation induced controlled Vickers crack growth in bending (ICVC), indentation strength in bending (ISB) of the tested composites.

The K_{IC} values obtained by the presented indentation methods are comparable. The alumina-10 wt% zirconia with unstabilized zirconia composite indicates the highest value of the fracture toughness independently on used methods. For this composite difference ranges within of 10%-20% for individual tested methods is noticed. Relationship of in-plane and out-of-plane displacements and strain distribution nearby Vickers hardness indentation at loading force 98.1 N and cracks with the K_{IC} was analysed by means of the interferometry method. Examples of in-plane displacement and strain in v(x,y) plane are shown on displacements and strain contour maps and 3D plots of displacement and strain for the Al_2O_3-10 wt% ZrO_2 with unstabilized zirconia composite (Fig.9, Fig.10).

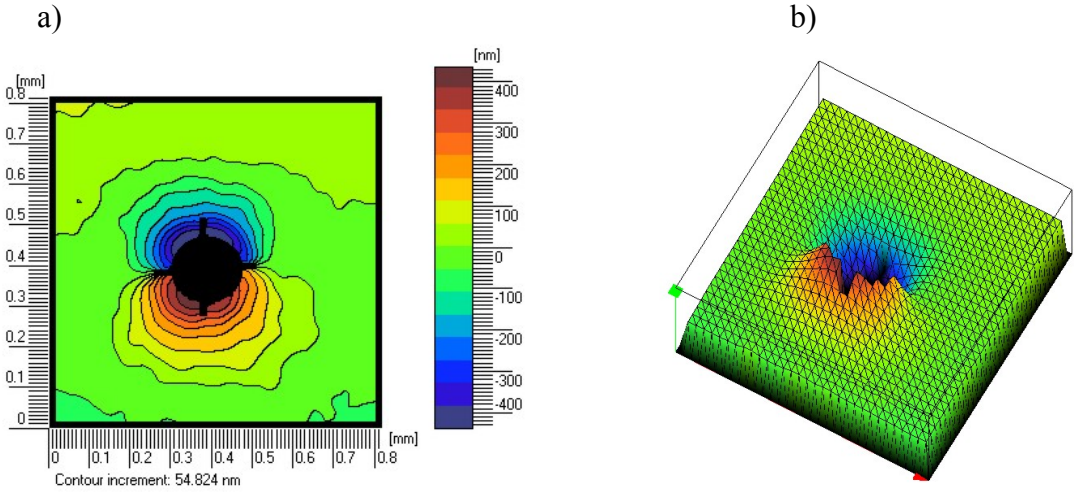

Fig.9. The analysis of v(x,y) in-plane displacement nearby Vickers indentation for the Al_2O_3-10 wt% ZrO_2 with unstabilized zirconia composite: a) contour map, b) 3D map of displacement distribution

In-plane displacements u(x,y) and v(x,y) achieve values placed within the range from 300 nm to 600 nm and their distribution is similar in both directions (Fig.9). Analysis of du/dx and dv/dx strains allows to observe distinct strain concentration at the end of the cracks (Fig.10).

a) b)

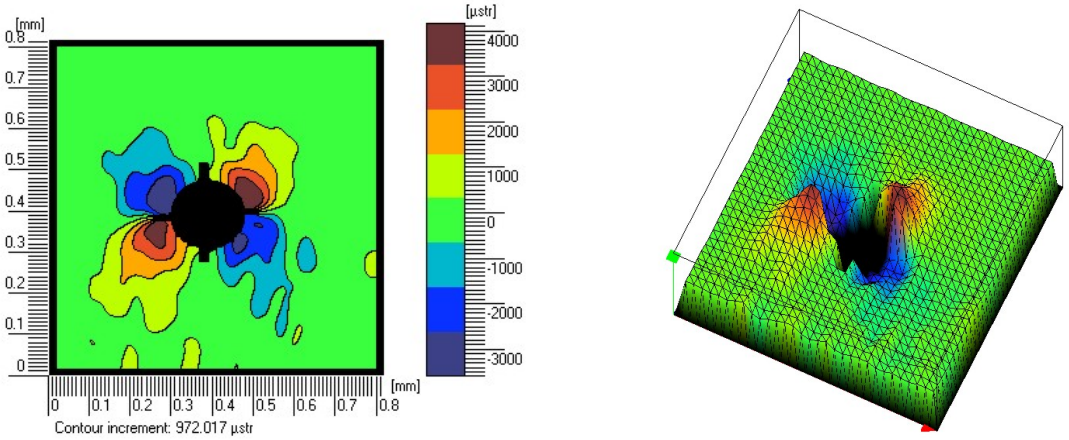

Fig.10. The analysis of in-plane dv/dx strain representing v(x,y) plane nearby Vickers indentation for the Al_2O_3-10 wt% ZrO_2 with unstabilized zirconia composite: a) contour map, b) 3D map of strain distribution

From the point of view of surface shaping in the zone of the Vickers hardness indentation the most interesting there are w(x,y) out-of-plane interferograms. On the basis of the analysis of the contour maps of w(x,y) out-of-plane displacements in the zone of the Vickers indentation for the alumina-10 wt% zirconia with 3 %mol yttria stabilized zirconia the maximum displacement (about 800 nm) were observed. This composite exhibits the smallest value of residual stress factor χ=0.063. However out-of-plane displacements for the other tested composites are smaller and are placed within range from 400 nm to 500 nm (Fig.11).

a) b)

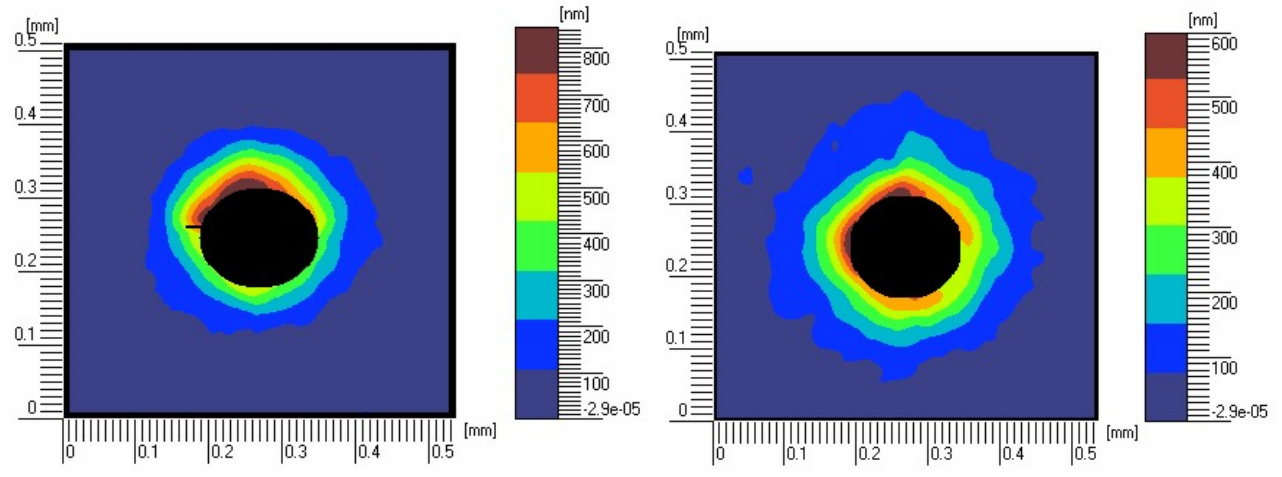

Fig.11. Images of contour maps of w(x,y) out-of-plane displacements nearby the Vickers hardness indentation for composites, a) Al_2O_3-10 wt% ZrO_2 with 3%mol yttria stabilized zirconia, b) Al_2O_3-30 wt% TiC+TiN with 2 wt% ZrO_2.

CONCLUSIONS

1. Fracture toughness determined according to various methods: indentation induced controlled Vickers crack growth in bending (ICVC), indentation strength in bending (ISB) and direct crack measurement (DCM) does not prove the significant difference.
2. Alumina-zirconia with unstabilized zirconia composite characterizes itself the highest fracture toughness from among tested ceramics.
3. Carried out calculations and own measurements allow on the verification and evaluation of the usefulness of the proposed methods in determining the K_{IC} for the most representative cutting tool ceramics.
4. Indentation technique has certain advantages compared with the conventional method because the experimental procedure is straightforward, involving minimal specimen preparation and small amount of material.

ACKNOWLEDGMENTS

Author sincerely thanks dr M. Boniecki at the Institute of Electronic Materials Technology and dr L.Sałbut at the Warsaw University of Technology for valuable experimental support.

References:

1. **Dusza J. and Steen M.,**"Brittle matrix composites: microstructure, room and high-temperature properties", The Proccedings of the International Conference DF PM'99, (1999), 277-288
2. **Riedel R.,** Handbook of ceramic hard materials,**1,2** Wiley-Vch, (2000)
3. **Warren P.D**., "Determining the fracture toughness of brittle materials by Hertzian indentation", J.Eur. Ceram. Soc.,**15** (1995), 385-394
4. **Muchtar A., Lim C.L. and Lee K.H.,** "Finite element analysis of Vickers indentation cracking processes in brittle solids using elements exhibiting cohesive post-failure behaviour", J.of Mater.Sci., **38** (2003), 235-243
5. **Szutkowska M. and Boniecki M.,** "Fracture toughness evaluation of Al_2O_3/TiC+TiN tool composite by means of controlled Vickers crack growth", J. Mater. Sci. Lett., **22** (2003), 1719-1721
6. **Chantikul P., Anstis G.R. et al.,** "A critical evaluation of indentation techniques for measuring toughness: II Strength method", J.Am.Ceramic.Soc., **64/9** (1981), 539-543
7. **Langford J., "**Indentation Microfracture in the Palmqvist crack regime:Implication for fracture Toughness evaluation by the Indentation method", J. Mater. Sci. Lett., **1** (1982), 493-495
8. **Niihara K. et al.,** "Futher reply to "Comment on elastic/plastic indentation damage in ceramics: The median /radian crack system", Communications of the Amer. Ceram. Soc., C-116 (1982)
9. **Laugier M.T.,** "New formula for indentation toughness in ceramics", J. Mater.Sci. Lett., **6** (1987), 355-356
10. **Anstis G.R., Chanticul P.,Lawn B.R., Marshall D.B.,** " A critical evaluation of indentation techniques for measuring fracture toughness. I Strength method", J. Amer. Ceram.Soc., 64/9 (1981),533-538
11. **Liang K.M., Orange G., Fantozzi G.,** "Evaluation by indentation of fracture toughness of ceramic materials", J. Mater. Sci**. 25** (1990), 207-214
12. **Lawn B.R., Fuller E.R.,** "Equilibrium penny-like craks indentation fracture", J. Mater. Sci.**10** (1975), 2016-2024
13. **Szutkowska M.,**"Fracture resistance behavior of alumina-zirconia composites", The Proceedings of the Inter. Conf.on Adv. in Mater. and Proc. Tech. AMPT 2003 in Dublin (2003), 1251-1254